Quasi-one-dimensional vortex matter in superconducting nanowires

W. Y. Córdoba-Camacho,[1,2] R. M. da Silva,[1] A. Vagov,[3,4] A. A. Shanenko,[1] and J. Albino Aguiar[1]

[1]*Departamento de Física, Universidade Federal de Pernambuco, Av. Prof. Aníbal Fernandes, s/n, 50740-560, Recife - PE, Brazil*

[2]*National Research University Higher School of Economics, 101000, Moscow, Russia*

[3]*Institut für Theoretische Physik III, Bayreuth Universität, Bayreuth 95440, Germany*

[4]*ITMO University, St. Petersburg, 197101, Russia*

(Received 28 December 2017; revised manuscript received 19 June 2018; published 26 November 2018)

It is well known that superconducting films made of a type-I material can demonstrate a type-II magnetic response, developing stable vortex configurations in a perpendicular magnetic field. Here we show that the superconducting state of a type-I nanowire undergoes more complex transformations, depending on the nanowire thickness. Sufficiently thin nanowires deviate from type I and develop multiquantum vortices and vortex clusters similar to intertype (IT) vortex states in bulk superconductors between conventional superconductivity types I and II. When the nanowire thickness decreases further, the quasi-one-dimensional vortex matter evolves towards type II so that the IT vortex configurations gradually disappear in favor of the standard Abrikosov lattice (chain) of single-quantum vortices. However, type II is not reached. Instead, an ultrathin nanowire re-enters abruptly the type-I regime while vortices tend to be suppressed by the boundaries, eventually becoming one-dimensional phase-slip centers. Our results demonstrate that arrays of nanowires can be used to construct composite superconducting materials with a widely tunable magnetic response.

DOI: 10.1103/PhysRevB.98.174511

I. INTRODUCTION

Low dimensional superconductors attract significant interest due to a tantalizing possibility to manipulate their properties by varying the sample geometry. A prospective example is recently fabricated arrays of superconducting nanowires (see, for instance, Refs. [1–7]) produced, e.g., by electrochemical deposition of a metal in a nanoporous insulating matrix or by the focused ion beams (FIB) lithography. Dimensional parameters of such acomposite superconducting material are controlled with high precision. As a result, one can tune the superconducting magnetic response that is a cornerstone characteristic of superconductors for their applications.

In particular, when a superconducting film made of a type-I material becomes sufficiently thin it can develop stable vortex configurations in a perpendicular magnetic field [8–10], becoming a type-II superconductor. This type of interchange takes place due to the stray magnetic field that introduces repulsion between initially attractive (and thus unstable) vortices. Extrapolating results for superconducting films to the case of a nanowire made of a type-I material in a perpendicular magnetic field, one expects that it can also become a type-II superconductor. Recent experiments [4] have indeed demonstrated that the magnetization of an array of superconducting nanowires changes notably when the wire thickness decreases. However, interpreting these changes is not straightforward. Indeed, extrapolating results for films must be taken with care. Nanowires are quasi-one-dimensional (1D) objects, where the condensate and its possible vortex-matter state are inevitably affected by the confining potential of the boundaries. If the boundary effects overcome the stray field influence, one can expect that a nanowire made of a type-I material remains a type-I superconductor irrespective of its thickness. Which of these factors actually dominates and whether a superconductivity type interchange can be observed in thin superconducting wires has not been investigated to date.

The present work fills this gap by studying the magnetic response of a single superconducting nanowire made of a type-I material. Our study demonstrates that sufficiently thin nanowires develop the mixed state in a perpendicular magnetic field. However, the related quasi-1D vortex matter is shown to exhibit vortex clusters and multiquantum vortices that are found in neither type II nor in type I but similar to IT vortex configurations in bulk superconductors [11–13]. When the nanowire thickness decreases further, vortices tend to arrange themselves in a regular chain (1D Abrikosov lattice) so that the system evolves towards type II. However, due to increasing 1D character of the sample, the type-II magnetic response is not reached. Instead, ultrathin nanowires re-enter the type-I regime: vortices start to become 1D phase-slip centers typical for 1D weak superconducting links [14] and are then expelled from the wire. We stress that our work differs fundamentally from earlier studies of the geometry related effects in small superconducting samples where vortices are confined in all dimensions and the geometry forces them to merge into clusters or multiquantum vortices. In contrast here the nanowire is assumed infinite (very long), vortices are not confined along it and thus the appearance of nonstandard IT configurations such as vortex clusters is not simply induced by the interaction with the boundaries.

II. MODEL AND METHOD

Our analysis is done on the basis of the GL theory. Although this approach cannot explain a finite IT domain in bulk superconductors [11], it is sufficient for systems where

the Bogomolnyi degeneracy is lifted due to geometry-related factors, as in the case of thin films, see Ref. [13] for a detailed discussion.

In the calculations we assume that a nanowire is in the form of a prism of the length L (in the z direction) and with the square cross section $d \times d$ (in the x and y directions) see Ref. [15]. The boundary condition for the order parameter Ψ on the wire surface is $[\mathbf{n} \cdot (-i\hbar\nabla - 2e\mathbf{A}/c)]\Psi = 0$, where $\mathbf{A}$ is the vector potential whose curl is the magnetic field $\mathbf{B} = \nabla \times \mathbf{A}$, and $\mathbf{n}$ is the unit vector perpendicular to the surface. We consider that $L \gg d$ and use the periodic boundary conditions with period L in the z direction for both Ψ and $\mathbf{B}$. The nanowire is placed in the perpendicular external homogeneous magnetic field $\mathbf{H} = (H, 0, 0)$, which implies an asymptotic condition $\mathbf{B} \to \mathbf{H}$ at infinity. In the calculations this condition is fulfilled on a surface of a larger embedding prism, also with the square cross section, with the surface located at distance $\Delta L = 10$ from the wire (hereafter all distances are given in the units of the bulk Cooper pair size ξ_0).

The GL equations for Ψ and $\mathbf{A}$ are solved using a standard method of auxiliary time dependence, where the time dependence is introduced by adding the first-order time derivatives of Ψ and $\mathbf{A}$ in the equations, such that the solution converges to the stationary point at sufficiently large times, see [15]. The resulting time-dependent equations are solved by using the link variable method [13,16].

The dimensionless GL equations for a nanowire depend on just two parameters: the GL parameter of the material $\kappa = \lambda/\xi$ (the ratio between the bulk GL coherence and magnetic lengths) and the nanowire thickness d. We choose $\kappa = 0.55$ which corresponds to a type-I material. This particular choice of κ is not essential as the results are qualitatively similar for any type-I material with $\kappa < 1/\sqrt{2}$. For this value of κ the main changes in the magnetic response take place when $d < 50$ and so we focus on this thickness interval. For clean superconductors with large bulk ξ_0 the length $d = 50$ can go far beyond the nanoscale. However, in practice the electronic mean free path, which is $\sim d$ [17], significantly reduces ξ_0 so that changes of the magnetic response are expected for the nanosize wires [4]. The external field is varied in the interval $0 < H < 0.5H_c(0)$, where $H_c(0)$ is the bulk thermodynamic critical field at zero temperature. To investigate the hysteresis in the magnetization, the calculations are done for the ascending and descending magnetic field, see details in [15]. Finally, we assume that $T = 0.7T_c$, where the GL theory is still applicable.

III. RESULTS

A summary of the results is shown in Fig. 1. Magnetization curves (the volume averaged value of $-4\pi M$ as a function of H), shown in Figs. 1(i) to 1(vi), correspond to the wire thicknesses $d = 50$, 20, 15, 10, 8, and 5, respectively. The upper magnetization curve (red circles) illustrates the ascending field case, the lower curve (blue circles) is the magnetization for descending field. The color density plots below each panel show the spatial distribution of $|\Psi|^2$ in the center cross-section plane of the wire perpendicular to the applied magnetic field, calculated for different representative points shown on the magnetization curve.

Figure 1(i) demonstrates results for a relatively thick wire with $d = 50$. Considering the ascending field magnetization curve together with the corresponding profiles of $|\Psi|^2$, one notes that the field does not enter the wire until the magnetization starts to decrease. This is a clear signature of the Meissner state. A decrease in $-4\pi M(H)$ indicates that the field penetrates the sample, where it forms the well-known intermediate state of type-I superconductors [18–20] with coexisting stratified normal and superconducting phases [see "b," "c," "d," and "e" in Fig. 1(i)]. The field occupies first the vicinity of the boundaries [see b in Fig. 1(i)], and then creates bubbles of the normal phase inside the superconducting condensate [see c in Fig. 1(i)]. The bubbles grow in size with increasing the field and then merge into a stripe, producing alternating normal and superconducting lamellas, see d in Fig. 1(i). Finally, the normal phase occupies almost the entire volume of the wire and superconductivity survives only near the boundaries [the surface superconductivity, see e and f in Fig. 1(i)]. Here lamellas are observed due to finite dimensions of the system. As the result, the magnetization does not drop to zero abruptly, as expected for type I in bulk but decreases gradually like in type-II materials.

The descending-field magnetization [blue curve in Fig. 1(i)] has a different sign (i.e., a paramagnetic response) and a much smaller absolute value. This is a hysteretic behavior, which takes place due to trapping of the magnetic flux inside the nanowire. For the descending field the intermediate state undergoes a similar sequence of patterns, however, in the reverse order as compared to the ascending field case [cf. a–f and A–E in Fig. 1(i)]. We note that for $d = 50$ the spatial field/condensate configurations has an effectively 2D character: the nanowire can accommodate more than one normal state bubble or stripe in its perpendicular direction [see c, d, A, and B in Fig. 1(i)]. It is also worth noting that when the field decreases, bubbles of the normal phase survive even in the limit $H \to 0$ due to the flux trapping, i.e., the system remains in a paramagnetic state at zero external field.

A wire with $d = 20$ is no longer a type-I superconductor, as seen from Fig. 1(ii). Here, similarly to Fig. 1(i), the interval on the ascending field curve (red) with increasing $-4\pi M$ corresponds to the Meissner state. However, the magnetization decrease is no longer smooth: it follows a sequence of sawlike drops. This is explained by looking at the density plots below, which demonstrates that unlike the case of $d = 50$ [cf. b in Fig. 1(i)], here the magnetic field penetrates the sample in the form of vortices. A drop in the magnetization occurs each time when additional vortices enter the wire, rearranging the vortex configuration [see a–e in Fig. 1(ii)].

However, Fig. 1(ii) does not exhibit standard type-II superconductivity either. An important difference is that at relatively small ascending fields (just after the Meissner state), the mixed state develops giant (multiquantum) vortices which are unstable in a type-II material [see b in Fig. 1(ii)]. Giant vortices are arranged in a 1D lattice (chain), and the magnetic flux carried by one vortex increases with the field (the vortices grow). When the external field exceeds a certain threshold, the multiquantum vortices are replaced by a chain of elongated clusters of single-quantum (Abrikosov) vortices [see c in Fig. 1(ii)]. By further increase of the field these clusters merge

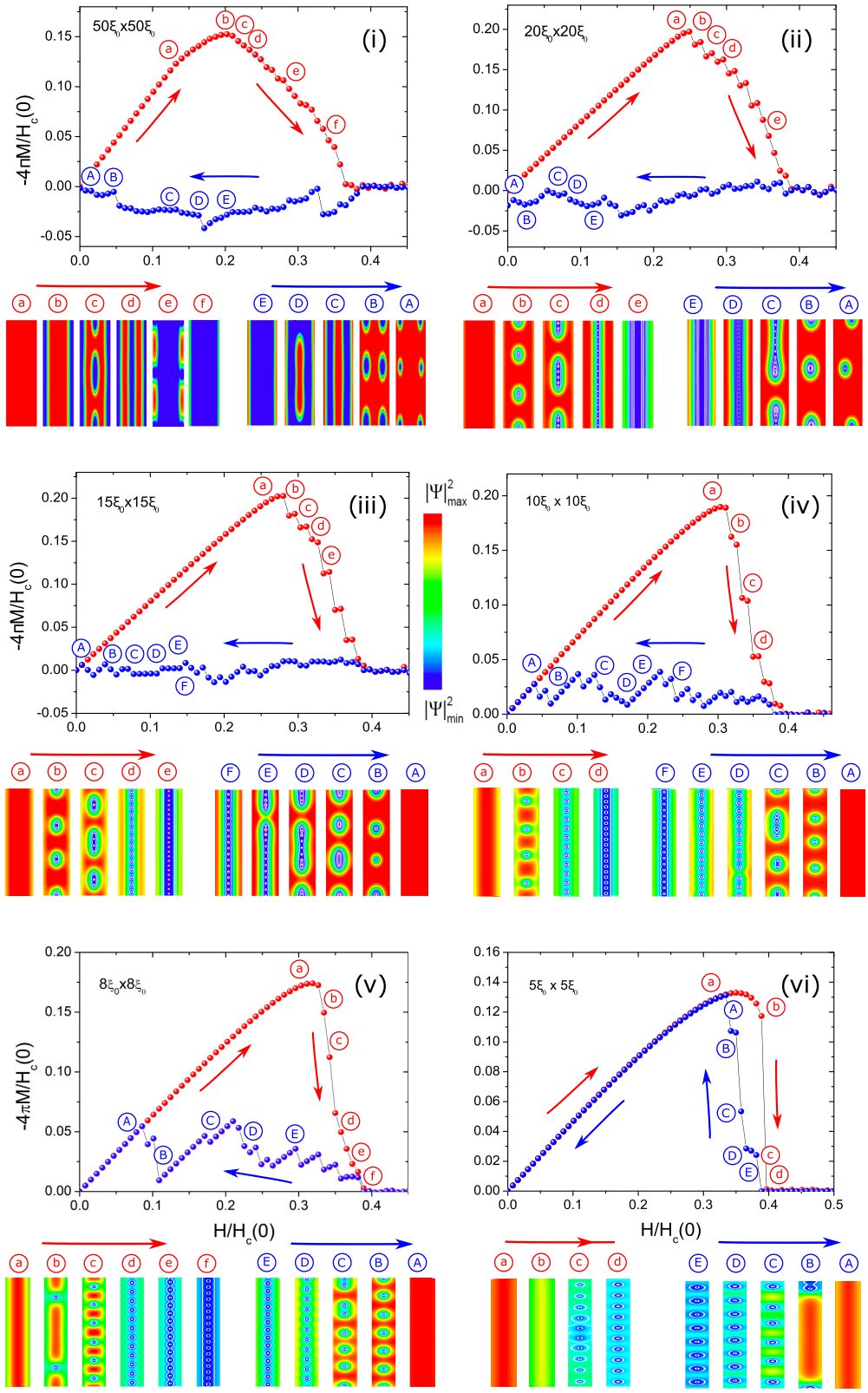

FIG. 1. Magnetization M ($-4\pi M$ is shown in the figure) as a function of the applied perpendicular magnetic field H for the wire with the square cross section $d \times d$: red points are results for the ascending field and blue points are for the descending field; panels (i), (ii), (iii), (iv), (v), and (vi) show results for $d = 50$, 20, 15, 10, 8, and 5 (in units of ξ_0). H and M are expressed in units of the bulk thermodynamic critical field $H_c(0)$ at $T = 0$. Density color plots below the magnetization panels demonstrate the spatial distribution of $|\Psi|^2$ calculated for the points displayed in the magnetization curves: small red letters a, b, c,... correspond to the ascending field magnetization and capital blue letters A, B, C, ... are for the descending field curve. Calculations are done at $T = 0.7T_c$ and bulk GL parameter $\kappa = 0.55$.

into a 1D lattice of single-quantum vortices located in the wire center [see d in Fig. 1(ii)]. Finally, at larger fields only surface superconductivity survives [see e in Fig. 1(ii)], before the superconducting state eventually disappears.

The field patterns seen in Fig. 1(ii) appear to be similar to those attributed earlier to the IT regime in bulk superconductors. This regime is found between conventional types I and II in the phase diagram for both single- and multiband superconductors [11,12]. Such nonstandard vortex configurations are related to a special vortex-vortex interaction that combines repulsion and attraction at different ranges and has a significant many-body (many-vortex) contribution favoring the formation of clusters [12] and giant vortices [11]. We expect that despite a strong boundary influence these IT features of the interaction between vortices are also present in nanowires. We note that this mechanism for the formation of giant vortices and vortex clusters is totally different from what is observed in small (mesoscopic) superconductors, where vortices are squeezed by the boundaries in all dimensions, see, e.g., [21–23]. A nanowire is an extended quasi-1D object where vortices can move freely along its length and their longitudinal arrangement is determined by the nontrivial interaction between them, rather than with boundaries. The infinite length implies that a system is in the thermodynamic limit so that one can still use the concept of superconductivity types.

For the descending field the plots of $|\Psi|^2$ in Fig. 1(ii) are similar to those of the ascending field case, though the sequence of patterns is reversed [cf. a–e with A–E in Fig. 1(ii)]. The descending-field magnetization is still negative, similarly to that in Fig. 1(i), but its amplitude becomes smaller, which indicates a weaker magnetic flux trapping. However, this is not the case in the limit $H \to 0$: the zero-field paramagnetic response (i.e., the paramagnetic Meissner effect) in Fig. 1(ii) is more pronounced then in Fig. 1(i). It should also be noted that a giant paramagnetic Meissner effect has previously been reported for bulk IT two-band superconductors [24].

The field-condensate patterns in Fig. 1(ii) are essentially of the 1D character (with the exception of A), in contrast with the 2D character of the density plots shown in Fig. 1(i). This can be viewed as the dimensional crossover in the mixed-state configuration. Surprisingly, the crossover occurs for values of d that are an order of magnitude larger than ξ_0.

For $d = 15$ [see Fig. 1(iii)] the magnetization is qualitatively similar to that of Fig. 1(ii). However, multiquantum vortices here play a minor role: they are absent for the ascending field case and visible only at point B on the descending field curve. However, clusters of single-quantum vortices observed at lower fields [see, e.g., b in Fig. 1(iii)] are still a clear signature of the IT superconductivity. The descending field curve still presents a paramagnetic Meissner response. However, its amplitude is much smaller then those observed in Figs. 1(i) and 1(ii). In the limit $H \to 0$ the residual magnetization goes to zero with no flux trapping.

Figures 1(iv) and 1(v) calculated, respectively, for $d = 10$ and $d = 8$, demonstrate that the nanowire is still in the IT regime, although in both ascending and descending cases giant vortices disappear. Vortex clusters are not seen at the ascending field but they are still present at the descending field [see C in Figs. 1(iv) and 1(v)]. One also sees that the descending and ascending magnetization curves become closer to one another. This can be explained by the decrease of the Bean-Livingston barrier [25], which makes it easier for vortices to escape the wire. The magnetization patterns in Figs. 1(iv) and 1(v) are apparently in agreement with the type II/1 concept of the IT superconductivity: the Abrikosov lattice at large fields is stable because of the short-range repulsion between single-quantum vortices, whereas clusters of vortices at smaller fields are explained by the long-range vortex attraction [26–32] (see also the discussion of type-II/1 configurations in the IT regime in Ref. [11]).

Finally, type II is almost approached at $d = 5$ [see Fig. 1(vi)]. Here the mixed state contains only single-quantum vortices arranged in a 1D Abrikosov lattice while the ascending and descending magnetization curves are very close to one another. However, in sharp contrast to type-II superconductors, the magnetization in Fig. 1(vi) almost instantly drops to zero when the field starts to penetrate the nanowire, so that the mixed state is restricted to a very narrow interval of the external field values. When decreasing the nanowire thickness further, vortices become energetically unfavorable and, finally, the system demonstrates a magnetic response of a type-I material. Surprisingly, the corresponding magnetization as a function of the applied magnetic field is close to that observed in bulk type-I superconductors, without any lamellas and bubbles of the normal state usually observed in finite samples. It is also worth noting that vortices in Fig. 1(vi) become elongated in the direction perpendicular to the nanowire. This is an onset of the formation of phase slip centers typical for 1D weak superconducting links [14].

IV. CONCLUSIONS

We have investigated the formation of quasi-1D vortex matter in a single nanowire made of a type-I material in a perpendicular magnetic field. It has been demonstrated that the magnetic response of the nanowire notably changes when its thickness decreases. Sufficiently thin nanowires deviate from type I in favor of the IT regime with multiquantum vortices and vortex clusters in the mixed state. In this case a regular chain of Abrikosov vortices is observed in the mixed state only when the field is close to its upper critical value. When decreasing the nanowire thickness further, signatures of the IT regime gradually disappear. However, the regime of type II superconductivity is not reached. Instead, ultrathin nanowires re-enter the type-I regime because the boundaries suppress the vortex matter. Although the calculations have been done for a single nanowire, our results are relevant for arrays of nanowires when they are sufficiently far from one another in an insulating template. This opens prospects of creating composite superconducting materials with widely tunable magnetic properties.

ACKNOWLEDGMENTS

This work was supported by the Brazilian agencies Coordenação de Aperfeiçoamento de Pessoal de Nível Superior (Grant No. 223038.003145/2011-00), Conselho Nacional de Ciência e Tecnologia (Grants No. 400510/2014-6 and No. 309374/2016-2), and FACEPE (APQ-0936-1.05/15). A.V. acknowledges the support from the Russian Science Foundation under the Project 18-12-00429 for studying the non-locality effects in vortex matter.

[1] J. S. Kurtz, R. R. Johnson, M. Tian, N. Kumar, Z. Ma, S. Xu, and M. H. W. Chan, Phys. Rev. Lett. **98**, 247001 (2007).

[2] T. G. Sorop and L. J. de Jongh, Phys. Rev. B **75**, 014510 (2007).

[3] Y. Zhang, C. H. Wong, J. Shen, S. T. Sze, B. Zhang, H. Zhang, Y. Dong, H. Xu, Z. Yan, Y. Li, X. Hu, and R. Lortz, Sci. Rep. **6**, 32963 (2016).

[4] K. O. Moura, K. R. Pirota, F. Béron, C. B. R. Jesus, P. F. S. Rosa, D. Tobia, P. G. Pagliuso, and O. F. de Lima, Sci. Rep. **7**, 15306 (2017).

[5] R. Córdoba, T. I. Baturina, J. Sesé, A. Yu Mironov, J. M. De Teresa, M. R. Ibarra, D. A. Nasimov, A. K. Gutakovskii, A. V. Latyshev, I. Guillamón, H. Suderow, S. Vieira, M. R. Baklanov, J. J. Palacios, and V. M. Vinokur, Nat. Commun. **4**, 1437 (2013).

[6] T. Morgan-Wall, B. Leith, N. Hartman, A. Rahman, and N. Marković, Phys. Rev. Lett. **114**, 077002 (2015).

[7] R. Córdoba, A. Ibarra, D. Mailly, and J. Ma De Teresa, Nano Lett. **18**, 1379 (2018).

[8] M. Tinkham, Phys. Rev. **129**, 2413 (1963).

[9] J. Pearl, Appl. Phys. Lett. **5**, 65 (1964).

[10] K. Maki, Ann. Phys. (NY) **34**, 363 (1965).

[11] A. Vagov, A. A. Shanenko, M. V. Milošević, V. M. Axt, V. M. Vinokur, J. A. Aguiar, and F. M. Peeters, Phys. Rev. B **93**, 174503 (2016).

[12] S. Wolf, A. Vagov, A. A. Shanenko, V. M. Axt, and J. A. Aguiar, Phys. Rev. B **96**, 144515 (2017).

[13] W. Y. Córdoba-Camacho, R. M. da Silva, A. Vagov, A. A. Shanenko, and J. A. Aguiar, Phys. Rev. B **94**, 054511 (2016).

[14] K. K. Likharev, Rev. Mod. Phys. **51**, 101 (1979).

[15] See Supplemental Material at http://link.aps.org/supplemental/10.1103/PhysRevB.98.174511 for the model and details of the numerical procedure.

[16] R. Kato, Y. Enomoto, and S. Maekawa, Phys. Rev. B **47**, 8016 (1993).

[17] M. Zgirski, K.-P. Riikonen, V. Touboltsev, and K. Yu. Arutyunov, Phys. Rev. B **77**, 054508 (2008).

[18] L. D. Landau, J. Exptl. Theoret. Phys. (JETF, USSR) **7**, 371 (1937).

[19] J. B. Ketterson and S. N. Song, *Superconductivity* (Cambridge University Press, Cambridge, 1999).

[20] P. G. de Gennes, *Superconductivity of Metals and Alloys* (Benjamin, New York, 1966).

[21] V. A. Schweigert, F. M. Peeters, and P. S. Deo, Phys. Rev. Lett. **81**, 2783 (1998).

[22] L. R. E. Cabral and J. Albino Aguiar, Phys. Rev. B **80**, 214533 (2009).

[23] J. Barba-Ortega, E. Sardella, J. Albino Aguiar, and E. H. Brandt, Physica C **479**, 49 (2012).

[24] R. M. da Silva, M. V. Milošević, A. A. Shanenko, F. M. Peeters, and J. Albino Aguiar, Sci. Rep. **5**, 12695 (2015).

[25] C. P. Bean and J. D. Livingston, Phys. Rev. Lett. **12**, 14 (1964).

[26] J. Auer and H. Ullmaier, Phys. Rev. B **7**, 136 (1973).

[27] M. Laver, E. M. Forgan, S. P. Brown, D. Charalambous, D. Fort, C. Bowell, S. Ramos, R. J. Lycett, D. K. Christen, J. Kohlbrecher, C. D. Dewhurst, and R. Cubitt, Phys. Rev. Lett. **96**, 167002 (2006).

[28] M. Laver, C. J. Bowell, E. M. Forgan, A. B. Abrahamsen, D. Fort, C. D. Dewhurst, S. Mühlbauer, D. K. Christen, J. Kohlbrecher, R. Cubitt, and S. Ramos, Phys. Rev. B **79**, 014518 (2009).

[29] S. Mühlbauer, C. Pfleiderer, P. Böni, M. Laver, E. M. Forgan, D. Fort, U. Keiderling, and G. Behr, Phys. Rev. Lett. **102**, 136408 (2009).

[30] E. H. Brandt and M. P. Das, J. Supercond. Nov. Magn. **24**, 57 (2011).

[31] A. Pautrat and A. Brûlet, J. Phys.: Condens. Matter **26**, 232201 (2014).

[32] T. Reimann, S. Mühlbauer, M. Schulz, B. Betz, A. Kaestner, V. Pipich, P. Böni, and C. Grünzweig, Nat. Commun. **6**, 8813 (2015).